

VII.14 A Novel Integrated Stack Approach for Realizing Mechanically Robust SOFCs

Scott A. Barnett (Primary Contact), Tammy Lai, Jiang Liu

Northwestern University

Dept. of Materials Science

2220 Campus Drive

Evanston, IL 60208

Phone: (847) 491-2447; Fax: (847) 491-7820; E-mail: s-barnett@northwestern.edu

DOE Project Manager: Lane Wilson

Phone: (304) 285-1336; E-mail: Lane.Wilson@netl.doe.gov

Objectives

- Develop a screen print process for fabricating integrated solid oxide fuel cells (SOFCs).
- Demonstrate that the process can provide the resolution and alignment required to fabricate integrated SOFCs with dimensions in the millimeter range.
- Determine the performance of integrated SOFC arrays, and make initial attempts to optimize them via materials processing.
- Predict the optimal dimensions for segmented-in-series SOFCs.

Approach

- Ceramic processes including powder pressing, screen printing, and high-temperature sintering were used to prepare zirconia supports and cell active layers with desired structures.
- Standard materials characterization techniques such as scanning electron microscopy (SEM) and x-ray diffraction (XRD) were utilized to determine if the desired phases and structures were achieved.
- Electrical testing methods such as impedance spectroscopy, commonly used for characterizing fuel cells, were employed.
- Electrical modeling was carried out using equations describing the resistance losses in individual cells and current flows in the supports, and equations were solved using the program MatLab.

Accomplishments

- Developed and demonstrated screen printing of all fuel cell components with the required resolution of <0.1 mm, desired microstructures (dense electrolytes and electrodes with porosity $>30\%$), and desired electrical properties.
- Demonstrated for the first time the successful operation of integrated solid oxide fuel cells with repeat periods of 1-2 mm, compared with 10 mm in prior work, and power densities in excess of 200 mW/cm^2 .
- Developed a detailed electrical model useful for design and optimization of segmented-in-series SOFCs. The model accounts for cell characteristics, electrode resistance losses, and substrate shunting currents. Optimal cell widths were predicted to be in the range of 2-3 mm, depending on the above factors.

Future Directions

No other work is planned on this project, but work is ongoing on other projects:

- We are continuing to evaluate different ceramic interconnect materials in order to achieve low resistance losses and high density using a process where the interconnect is co-sintered with the other key cell

components. This is a key for achieving simple processing, low materials cost, and optimal cell performance.

- Work is still ongoing to analyze cell test results as a function of electrode sheet resistance in terms of the model. This will allow us to validate the model, make more quantitative predictions, and better predict optimal geometries/materials. At the same time, component processing and structure are being improved in order to achieve better stack performance.
- The work should also be extended to larger area devices with larger numbers of integrated cells. There are no fundamental issues here, but this will require detailed attention to processing in order to achieve flat surfaces and uniform properties across large wafers.

Introduction

While great success has been achieved with high-performance individual planar solid oxide fuel cells (SOFCs), problems remain with interconnecting, stacking, and sealing these devices to make full-scale generators. Some of these problems may continue, for some time to come, to be significant barriers to achieving reliable, low-cost, long-lived SOFC generators. Thus, other approaches should be explored that have the potential to circumvent these problems. This was the rationale behind the present project, in which we explored a novel segmented-in-series stack geometry. The segmented-in-series design is shown schematically in Figure 1. The geometry features an integral ceramic interconnect that avoids oxide scale problems with metallic interconnects, a flattened tubular design that provides for easier sealing while maintaining high power densities, and small-width cells that minimize current collection losses.

Considerable progress was made during this project. The entire materials processing sequence was developed and successfully implemented. Initial devices were fabricated, characterized, and successfully tested. A model was developed to explain the device performance results and to allow

for prediction of optimal device design for future work. The results of this preliminary work are extremely promising, and we believe that this approach merits increased development efforts. The approach should provide for much better sealing than planar designs, and thus should be very useful for hydrogen generation schemes such as steam electrolysis.

Approach

Our approach combined experimental work and modeling. The experimental work was mainly to demonstrate the feasibility and utility of the novel stack geometry and to provide initial process and materials development for future work. The modeling was to help understand the experimental device performance and to provide a design tool for future development.

Experimental Results

Baseline studies were carried out to determine materials processing conditions that yielded the desired material structures and properties. A design-of-experiments study of partially-stabilized zirconia (PSZ) supports was carried out to obtain optimal strength for desired porosity levels of 30-40%. Based on the results, cell fabrication was done on PSZ supports with a filler content of 15 wt%, with strengths of ≈ 150 MPa.

In order to achieve low ohmic losses in mm-wide devices, the sheet resistance of electrodes should be $< \approx 10$ /square. The sheet resistance of single Ni-YSZ (yttria-stabilized zirconia) screen-printed layers (≈ 10 m thick) was $0.2\text{--}0.25$ Ω /square from 600°C – 800°C , well below the desired value. Thus, single Ni-YSZ

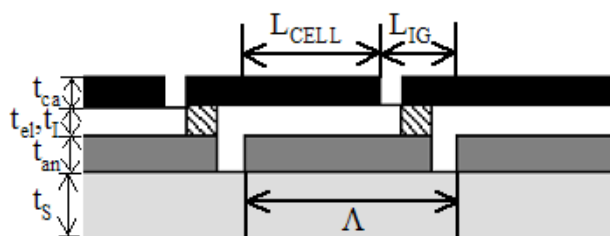


Figure 1. Cross-Sectional Schematic of the Segmented-in-Series Geometry

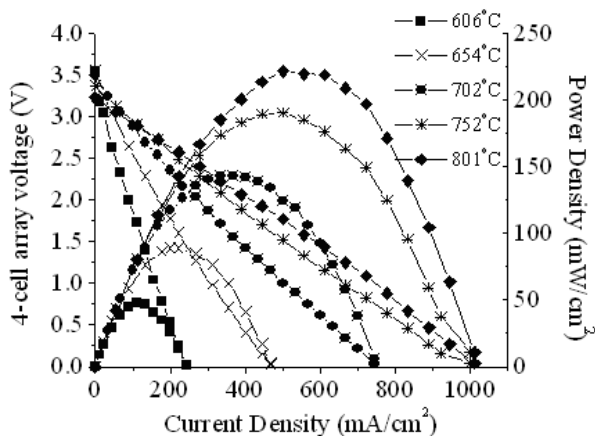


Figure 2. Voltage and Power Density versus Current Density for a Four-Cell SOFC Array Tested in Air and Humidified Hydrogen at Various Temperatures

printed layers provide negligible contribution to the array resistance.

The Ni-YSZ conductivity was ≈ 1000 S/cm, in fairly good agreement with literature values.¹

The cathodes consist of an LSCF-GDC layer printed directly on the electrolyte followed by a strontium- and iron-doped lanthanum cobaltite (LSCF) layer, both fired at 950°C . The LSCF-GDC layer provides good electrochemical performance,² but the low electronic conductivity of the gadolinium-doped ceria (GDC) component results in a high sheet resistance. The LSCF layer is used to provide an acceptable sheet resistance. LSCF sintered at 950°C yielded $r_s = 12$ /square at 800°C , corresponding to a conductivity of ≈ 70 S/cm in the $10\text{--}15$ μm thick layer. This is considerably lower than literature values for dense LSCF,³ perhaps due to the porous structure. Nonetheless, the single LSCF layer sintered at 950°C yielded a sheet resistance near the desired range of ≈ 10 /square.

Cross-sectional SEM was used to view the microstructures of the various layers after cell testing. In general, the microstructures were as expected. The Ni-YSZ layer was typically ≈ 15 μm thick and was porous with an average particle size of ≈ 1 μm . The YSZ layer was a double print, reasonably dense but with some closed porosity, typically $\approx 20\text{--}30$ μm thick. Thinner electrolytes can

presumably be used when a denser electrolyte structure is achieved. The cathode bi-layer was ≈ 30 μm thick with a porous structure (≈ 0.5 μm particle size), good adhesion to the electrolyte, and no clear evidence of the interface between the LSCF-GDC and LSCF layers.

Cell tests were carried out with air at the cathode and humidified hydrogen fed through the tube to the anode. The results of a typical four-cell array test are given in Figure 2. Open circuit voltages (OCV) ranged from 3.22–3.55 V, well below the theoretical value of ≈ 4.4 V. The porosity in the electrolyte and interconnect layers (SEM observation of the Pt and Au interconnects showed large porosity) is likely the dominant cause of the low OCV. Our calculations, described below, indicate that the PSZ support shunting current was too small to significantly reduce the OCV. The maximum power density calculated using the full array area was >200 mW/cm^2 at 800°C .

Both Au and Pt interconnects were tested, as well as $\text{Sr}_{0.94}\text{Y}_{0.04}\text{TiO}_3$ and $\text{Sr}_{0.55}\text{La}_{0.30}\text{TiO}_3$. The metallic interconnects yielded similar results as shown above. The La-doped interconnect was tested and gave almost no power output. The Y-doped interconnect gave only ~ 12 mW/cm^2 . It appears that the air conductivity of the doped SrTiO_3 is very low, preventing sufficient current flow through the interconnect. Other ceramic interconnect compositions are under investigation under other funding, and the results are very promising.

Calculation Results

Resistance-loss calculations were applied to realistic segmented-in-series geometries. The surface can be divided into active cell width L_{CELL} and interconnect/gap width L_{IG} . We have assumed interconnect/gap widths that are fixed by processing considerations. For example, in screen printing, there are limitations on resolution and print-to-print alignment. Relatively generous widths were chosen to provide easy alignment, i.e. wide gap widths (0.25 mm for the anode and 0.5 mm for the cathode) and relatively wide interconnects (0.5 mm), yielding a total inactive area $L_{\text{IG}} = 1.25$ mm. These values are well above the limits achievable by screen printing: ≈ 0.1 mm. The interconnect conductivity used was

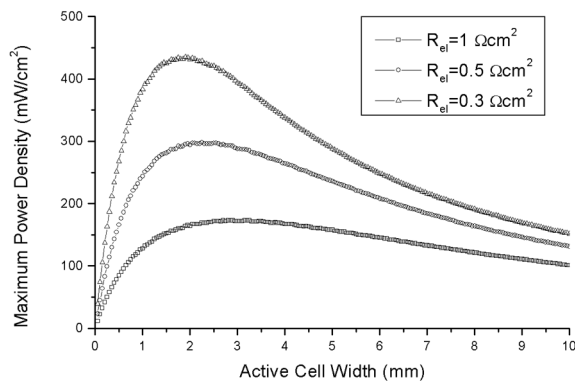


Figure 3. Maximum Power Density versus Active Cell Width L_{CELL} for a Segmented-in-Series Array

1 S/cm, a conservative value for typical ceramic interconnect materials such as doped LaCrO_3 . The cathode was taken to have a sheet resistance of 4 cm^2 .

Figure 3 shows the maximum power density versus active cell width for each of three different assumed area specific resistance (ASR) values. The curves each show a maximum power density at a different optimal L_{CELL} value. For cells with a relatively low ASR of $0.3 \text{ } \Omega\text{cm}^2$, the maximum power is 0.43 W/cm^2 at $L_{\text{CELL}} = 1.75 \text{ mm}$. For cells with a relatively high ASR of $1.0 \text{ } \Omega\text{cm}^2$, the maximum power is 0.17 W/cm^2 at $L_{\text{CELL}} = 2.9 \text{ mm}$. Note that if a smaller gap width L_{IG} is assumed, then the optimal cell widths shift to lower values and the maximum power densities to higher values. In general, the maximum results from the competition of two factors. First, at large cell widths, the electrode lateral resistance becomes large, yielding very low power densities. Second, as the cell width decreases to low values, the fraction of the total area taken up by the interconnect/gap area dominates, yielding low power.

We also carried out a detailed calculation of the shunting current in a mildly conducting support material for the segmented-in-series geometry. In order to provide a specific example of the shunting current expected in a typical segmented-in-series SOFC, we have assumed PSZ supports. Resistivity values for dense PSZ range from 1075-415 cm between 600-1000°C, respectively. These values were corrected to reflect the actual resistivity of the real supports, accounting for the typical porosity of

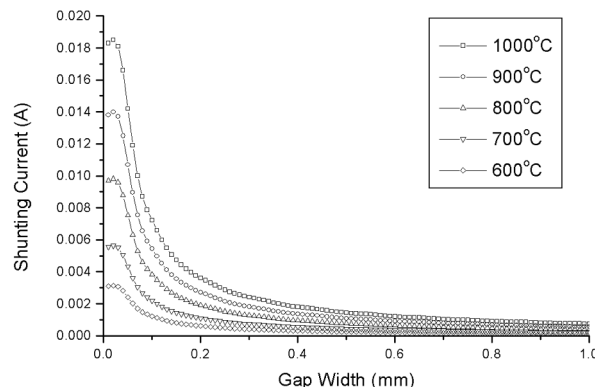


Figure 4. Shunting Current in a Porous PSZ Support versus Anode Gap Width for Different Operating Temperatures

$\approx 40 \text{ vol}\%$. Since PSZ is ionically conducting and the Ni-YSZ electrodes are electronically conducting, current flow through the support must involve electrochemical reactions at each of the interfaces and an associated polarization resistance. This resistance is neglected in the present calculation because its value may vary greatly depending on exact electrode composition and structure. Thus, the shunting current values given below must be regarded as upper limits.

Figure 4 shows a plot of the normalized current across a gap as a function of the gap width. Note that the current increases with decreasing gap width because of the increasingly high local current density as the gap narrows. Average shunting currents decreased rapidly for gap widths increased from 0 to 0.1 mm, after which they decreased more gradually. Taking the anode gap width of 0.25 mm assumed above, the shunting current should not be more than 2 mA at 800°C, or less than 2% of the total cell current (see Figure 4). Even for the smallest anode gap widths one might use, e.g. 0.1 mm, the shunting current is relatively small at 800°C. It is only at higher temperatures and small widths that the shunting current can become important. Shunting currents of this magnitude will not significantly affect the open-circuit voltage or maximum power density.

Summary and Conclusions

Millimeter-scale segmented-in-series SOFC arrays have been fabricated and tested. Optimization of the substrate processing, structure, and strength

were carried out, and screen printing inks and printing conditions were developed to achieve desired component structures. Fabrication of all patterned active layers by screen printing and co-sintering was successfully demonstrated. Electrical testing of four-cell arrays showed reasonable power densities for an initial study. There is considerable potential to improve upon this performance by increasing the fractional active cell area, increasing the OCV values, and reducing electrode polarization losses via improved active layer structures. The devices demonstrated here, containing only four cells in series on planar supports, are just an initial demonstration. When these devices are implemented on flattened tubes, they will combine most of the advantages of tubular SOFCs, i.e. integral interconnect and minimal sealing issues, with those of planar SOFCs, i.e. high power-to-volume ratio and ease of fabrication.

Calculations of the losses in segmented-in-series arrays, including electrode resistances, interconnect resistance, and shunting by a weakly conducting support material, show that millimeter-scale devices have advantages compared with the typical centimeter-wide cells. The results show that for $\approx 20\text{ }\mu\text{m}$ thick electrodes and interconnects and lateral print accuracy of $\approx 200\text{ }\mu\text{m}$, maximum power densities are achieved for cell widths of 2.9 to 1.75 mm as the cell resistance is decreased from 1 to $0.3\text{ }\Omega\text{cm}^2$. Shunting currents were found to have little effect on power density assuming partially-stabilized zirconia supports at temperatures below $\approx 800^\circ\text{C}$.

References

1. N.Q. Minh, *J. Am. Ceram. Soc.* **76**, 563-88 (1993).
2. E.P. Murray, M.J. Sever and S.A. Barnett, *Solid State Ionics* **148**, 27-34 (2002).
3. S.J. Skinner, *Intl. J. Inorg. Mater.* **3**, 113-121 (2001).

FY 2004 Publications/Presentations

1. T.S. Lai, J. Liu, and S.A. Barnett, "Patterned series-connected SOFCs," in Solid Oxide Fuel Cells VIII, Ed. By S.C. Singhal and M. Dokiya, (Electrochem. Soc., Pennington, NJ, 2003) p. 1068-1076.
2. T.S. Lai, J. Liu, and S.A. Barnett, "Effect of cell width on segmented-in-series solid oxide fuel cells," *Electrochem. Solid State Lett.* **7**, A78-A81 (2004).

Special Recognitions & Awards/Patents Issued

1. "Direct Hydrocarbon Fuel Cells" 6,479,178 (CIP covers basic cell design).